770-R-2

PRE-SUNRISE CHANGES IN VLF RADIO WAVES IONOSPHERICALLY REFLECTED NEAR VERTICAL INCIDENCE-II

January 1966

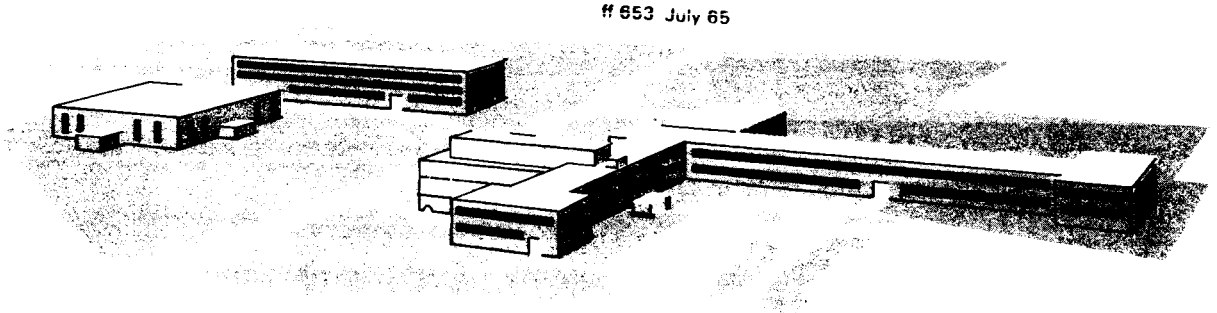

HRB

H R B - S I N G E R , I N C .

SCIENCE PARK · STATE COLLEGE, PENNSYLVANIA

A S U B S I D I A R Y C O M P A N Y

HRB-SINGER, INC.
A SUBSIDIARY OF THE SINGER COMPANY
Science Park, State College, Pa.

770-R-2

PRE-SUNRISE CHANGES IN VLF RADIO WAVES IONOSPHERICALLY REFLECTED NEAR VERTICAL INCIDENCE-II

Contract No. NASW-1109
National Aeronautics and Space Administration
Washington, D.C.

January 1966

Copy No. 1 of 45 Copies

Prepared By:

J. M. Musser

Approved By:

A. F. Lopez, Director
Intelligence Systems Laboratory

ABSTRACT

N66186 49

This report describes the results of a continued program of measurement of the down-coming skywave of Navy VLF station NSS as received at Wallpps Island, Virginia. These measurements, in cooperation with the University of Illinois and its D-region rocket experiments, have detected the development of the C-region of the ionosphere before ground sunrise.

author

Reverse (Page iv)Blank

TABLE OF CONTENTS

Reverse (Page vi) Blank

LIST OF ILLUSTRATIONS

Reverse (Page viii) Blank

A. INTRODUCTION

VLF recordings of the amplitude and relative phase of the components of the down-coming skywave of NSS (21.4 Kc/s) have been made at Wallops Station, Virginia from June to December of 1965. These measurements have been carried out to complement D-region rocket experiments conducted at sunrise and sunset by Professor S. A. Bowhill of the University of Illinois.

Typical sunrise recordings of the abnormal component are presented to illustrate the variability of the C-region of the ionosphere. Interpretations of the mechanisms involved are suggested.

A computer program for full-wave analysis of steep-incidence VLF propagation is being prepared and is briefly described. As it is still in the "debugging" stage, no numerical results are presented.

Reverse (Page 2) Blank

B. EXPERIMENTAL TECHNIQUE

The wave emitted from a VLF transmitter (e.g., NSS at 21.4 kc/s) with a vertical antenna is polarized with its electric vector parallel to the plane of incidence. After reflection, however, it is elliptically polarized with components both parallel and perpendicular to the plane of incidence.

The electromagnetic field at a receiver on the ground is composed of a linearly polarized ground wave and the elliptically polarized downcoming skywave. The skywave may be split into two linearly polarized components: the normal component, like the ground wave, has the magnetic vector (H_1) horizontal; the abnormal component has the electric vector (E_2) horizontal. The various field components are shown in Figure 1, where subscripts are 0 for ground wave, 1 for normal component of the skywave, and 2 for the abnormal component.

The measurable quantities are H_N, the total normal component, and H_A, the abnormal component, of the horizontal magnetic field expressed as:

$$H_N = H_0 + 2H_1$$

$$H_A = 2H_2 \cos \theta$$

The factor $2H_1$ is the normal component of the skywave, doubled because of reflection at the ground; the factor $2H_2 \cos \theta$ is the horizontal component of the abnormal incident and ground-reflected waves. See Figures 1b. and 1c.

The amplitudes of the components of the downcoming skywave relative to the incident field amplitudes are denoted by the reflection coefficient $\|R\|$ and conversion coefficient $\|R_\perp$. These may be calculated from the equations

$$\|R\| = \frac{H_1}{H_0} \cdot \frac{S}{d \sin \theta}$$

$$\|R_\perp = \frac{H_A}{H_0} \cdot \frac{S}{2d \sin \theta \cos \theta}$$

where d/S is the ratio of the paths traversed by the ground wave and one-hop skywave.

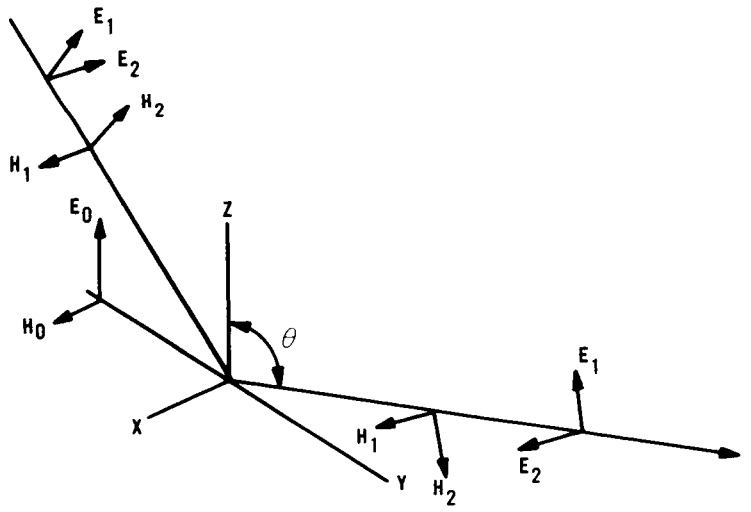

(A)

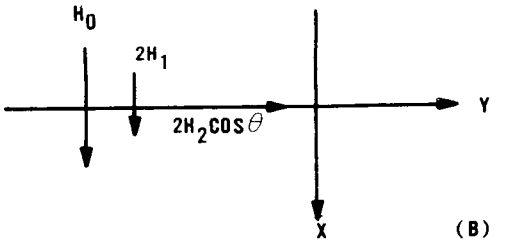

(B)

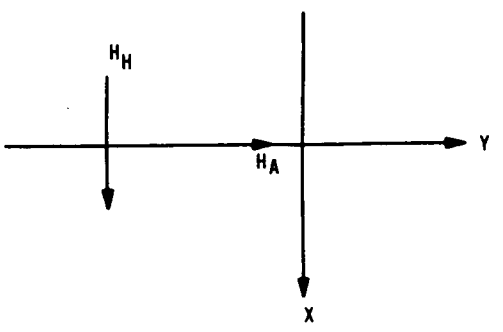

(C)

FIG. 1 COMPONENTS OF THE FIELD AT THE GROUND (BRACEWELL, 1952)

In order to measure the amplitude and phase of either component in the presence of a much stronger ground wave, it is necessary to separate the two fields. To isolate the abnormal component, H_2, it is necessary to use a well-designed loop antenna with its plane perpendicular to the plane of incidence; it will produce an emf proportional to H_A.

If it is desired to observe the normal component, H_1, a loop antenna is positioned so that its plane is in the plane of incidence and it receives an emf proportional to

$$H_N = H_0 + 2H_1.$$

A vertical whip antenna receives an emf proportional to

$$[E_0 + 2E_1 \sin \theta] \propto [H_0 + 2H_1 \sin \theta].$$

These two antenna voltages may be added in the appropriate phase and amplitude so as to eliminate E_0 and leave in the combined antenna system an emf proportional to

$$2H_1 (1 - \sin \theta).$$

Reverse (Page 6) Blank

C. EXPERIMENTAL RESULTS

Recordings of the amplitude and relative phase of NSS have been made at Wallops Station continually during the months of June - July and October - November - December, 1965. During August - September, 1965, the receivers and transmitter were both down for maintenance and repair. During the periods of recording, the abnormal component has been studied extensively. Specifically, pre-sunrise decreases in the abnormal amplitude have been studied. This has resulted in the detection of three mechanisms which occur before ground sunrise.

The sunrise transitions have been categorized by similarities in onset time of a decrease of abnormal amplitude, as well as by the rate and amount of decrease of the amplitude. This has resulted in five categories; a typical day from each category is shown in Figures 2 to 6. Both a diagram of amplitude and phase as a function of time and a polar diagram are presented. Decreases in abnormal amplitude begin at three separate zenith angles, $\chi = 99^{\circ}$ to 100°, $\chi = 97^{\circ}$ to 98°, and $\chi = 94^{\circ}$. An amplitude decrease may begin at any of the above onset times or any combination of the above.

Figure 2 is representative of those sunrise transitions having a step-like decrease in amplitude occurring when the zenith angle is between 95° and 93°, with the amplitude then remaining nearly constant until about ground sunrise ($\chi = 90^{\circ}$). The decrease in amplitude occurs during a period of nearly constant phase. The magnitude of this step is of the order of 4db and may be preceded by a slow decrease beginning either near $\chi = 99^{\circ}$ or 97°.

An example of attenuation showing complete solar control is shown in Figure 3. The amplitude begins to decrease at $\chi = 97^{\circ} - 98^{\circ}$. It continues to decrease monotonically until $\chi = 90^{\circ}$ where the onset of the sunrise phase advance indicates that the attenuation is no longer non-deviative. This attenuation varies from 6 to 12 db.

Figure 4 represents transitions similar to Figure 3, demonstrating complete solar control; however, the onset time of the attenuation is delayed beyond $\chi = 98^{\circ}$ to as late as $\chi = 93^{\circ}$. The onset varies from $\chi = 93^{\circ}$ to 95°.

The sunrise recording of 14 June 1965 has been chosen to represent the next group as this was the date of a D-region rocket experiment by the University of Illinois (Figure 5). This transition is characterized by a slow decrease in

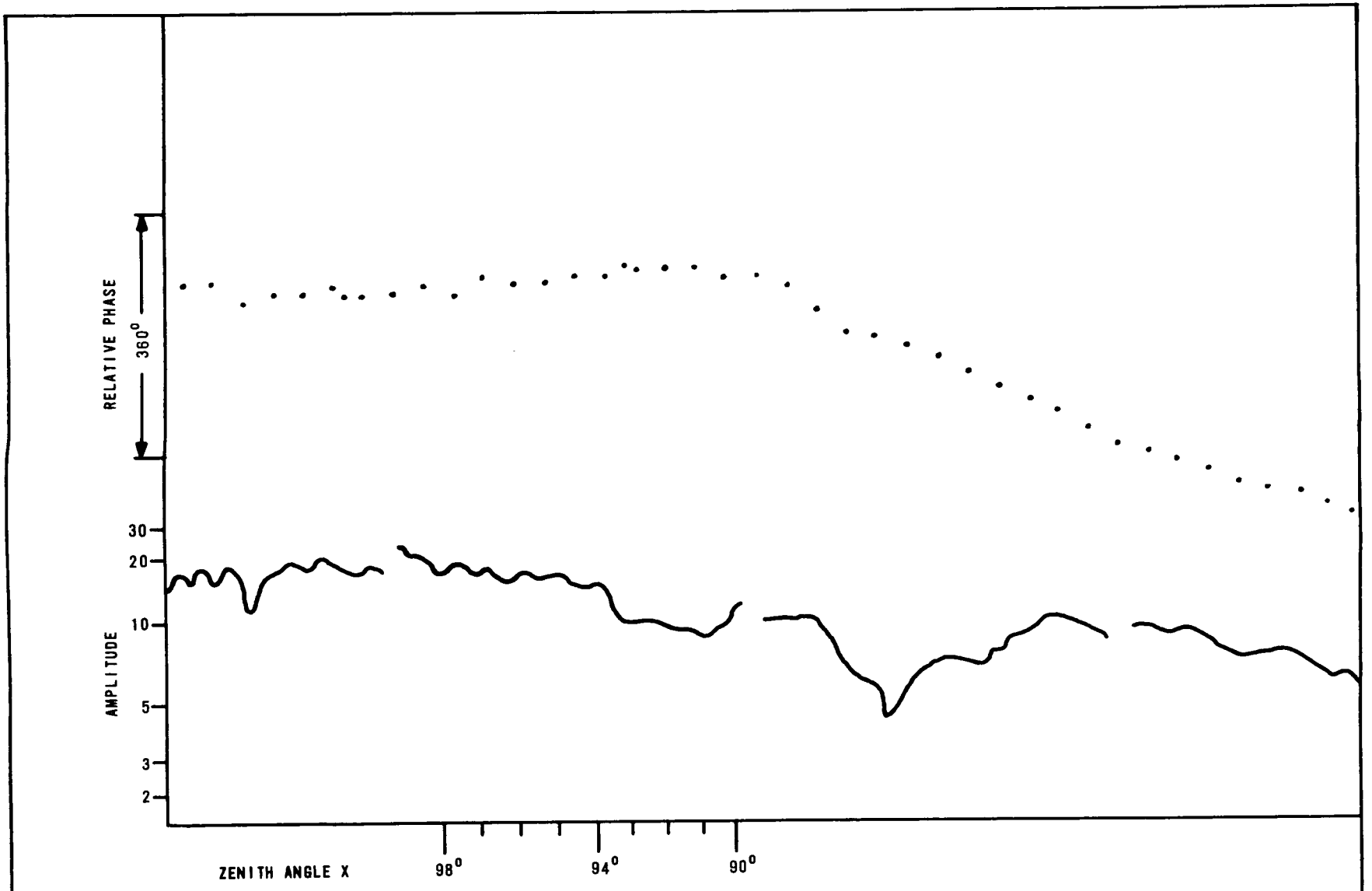

FIG. 2A ABNORMAL COMPONENT FOR JULY 22, 1965 SUNRISE

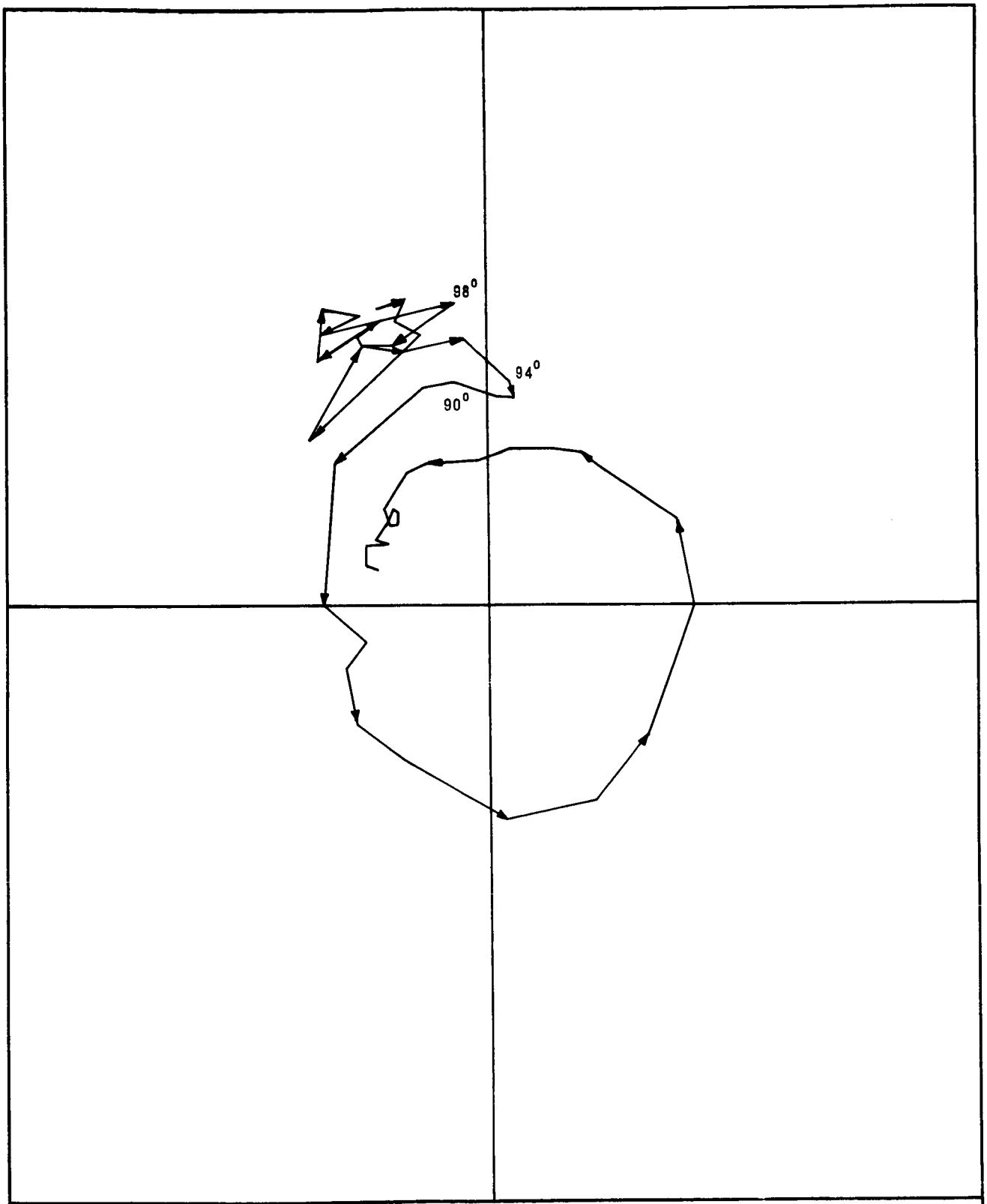

FIG. 2B ABNORMAL COMPONENT FOR JULY 22, 1965 SUNRISE

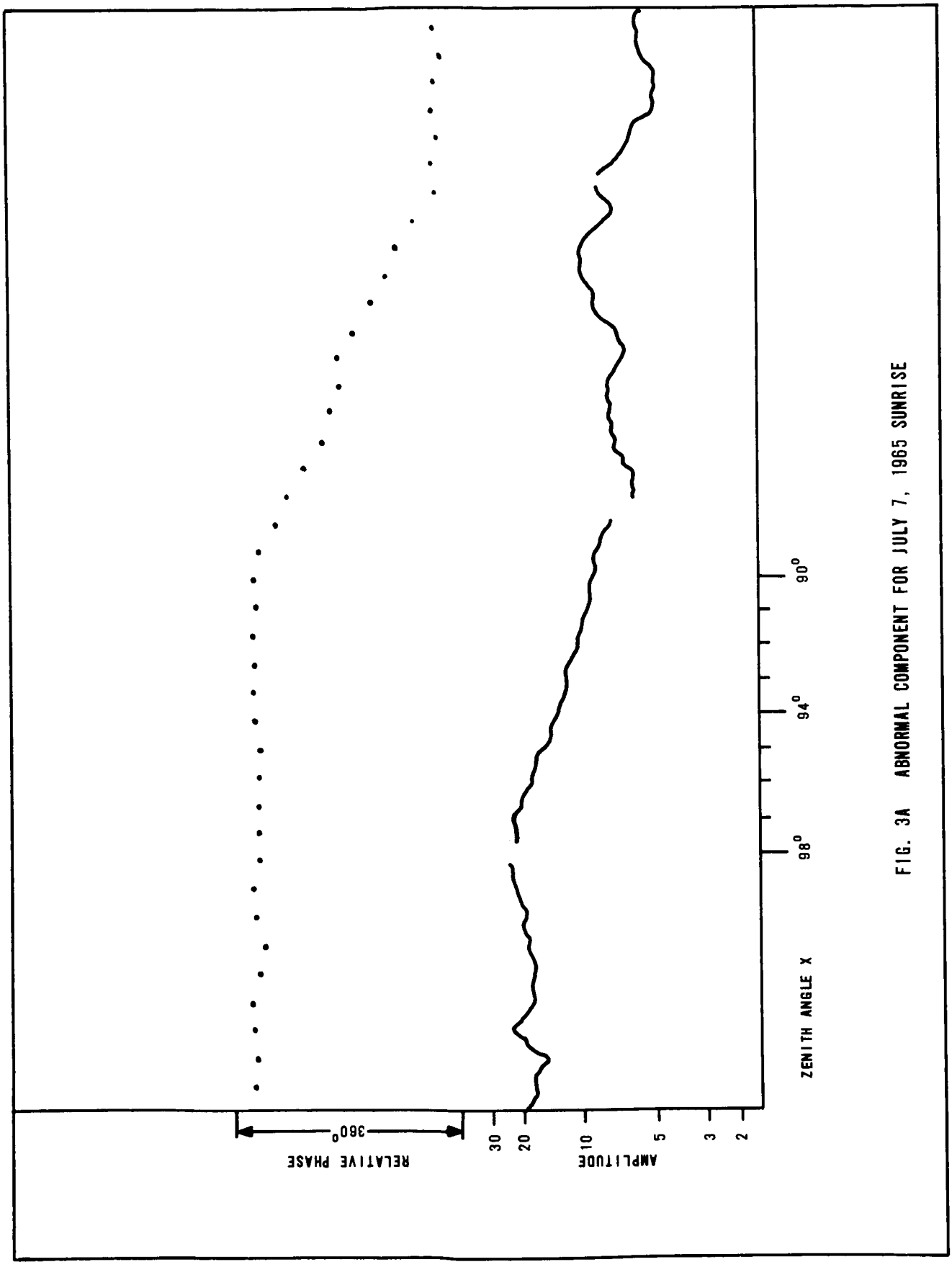

FIG. 3A ABNORMAL COMPONENT FOR JULY 7, 1965 SUNRISE

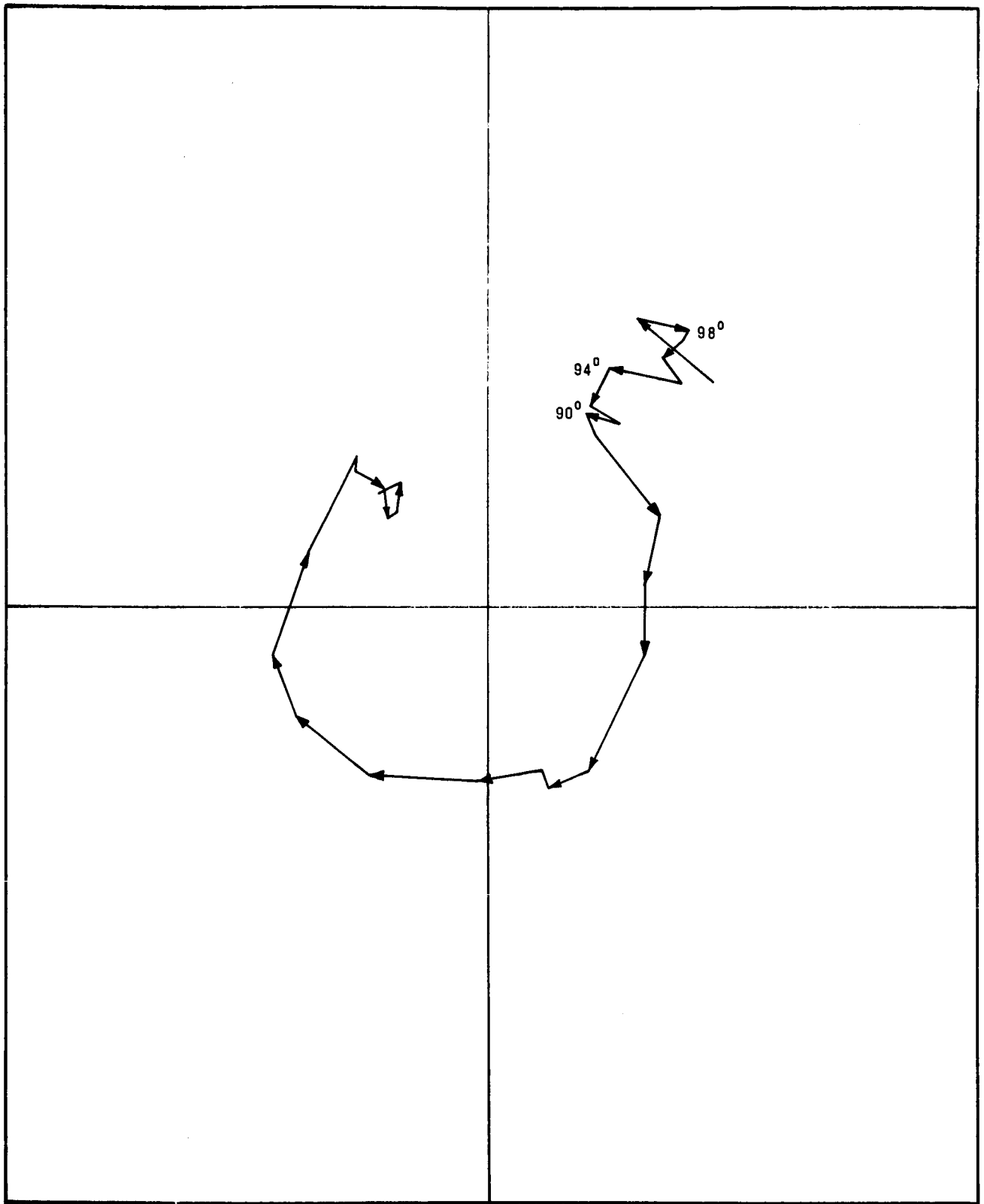

FIG. 3B ABNORMAL COMPONENT FOR JULY 7, 1965 SUNRISE

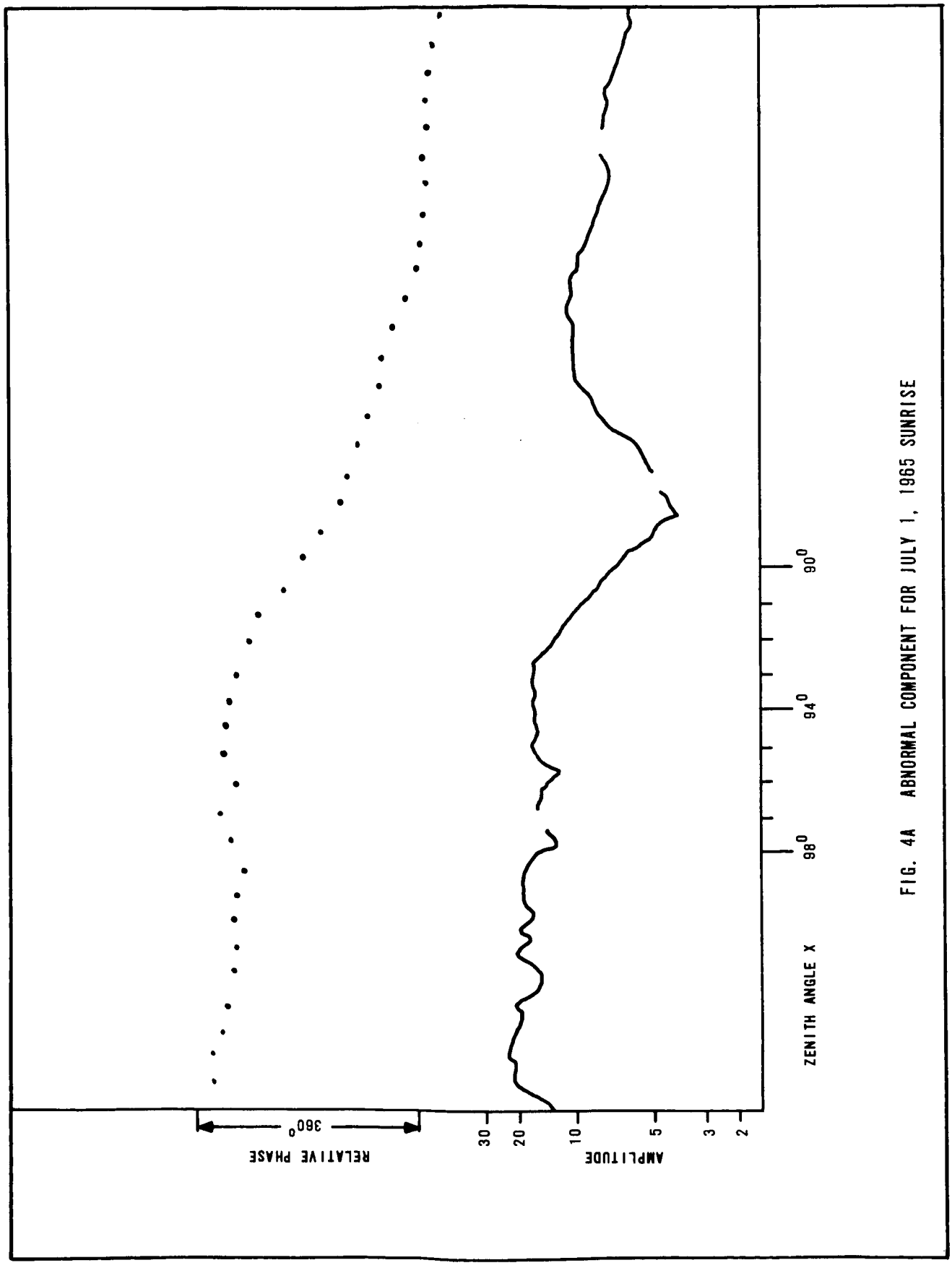

FIG. 4A ABNORMAL COMPONENT FOR JULY 1, 1965 SUNRISE

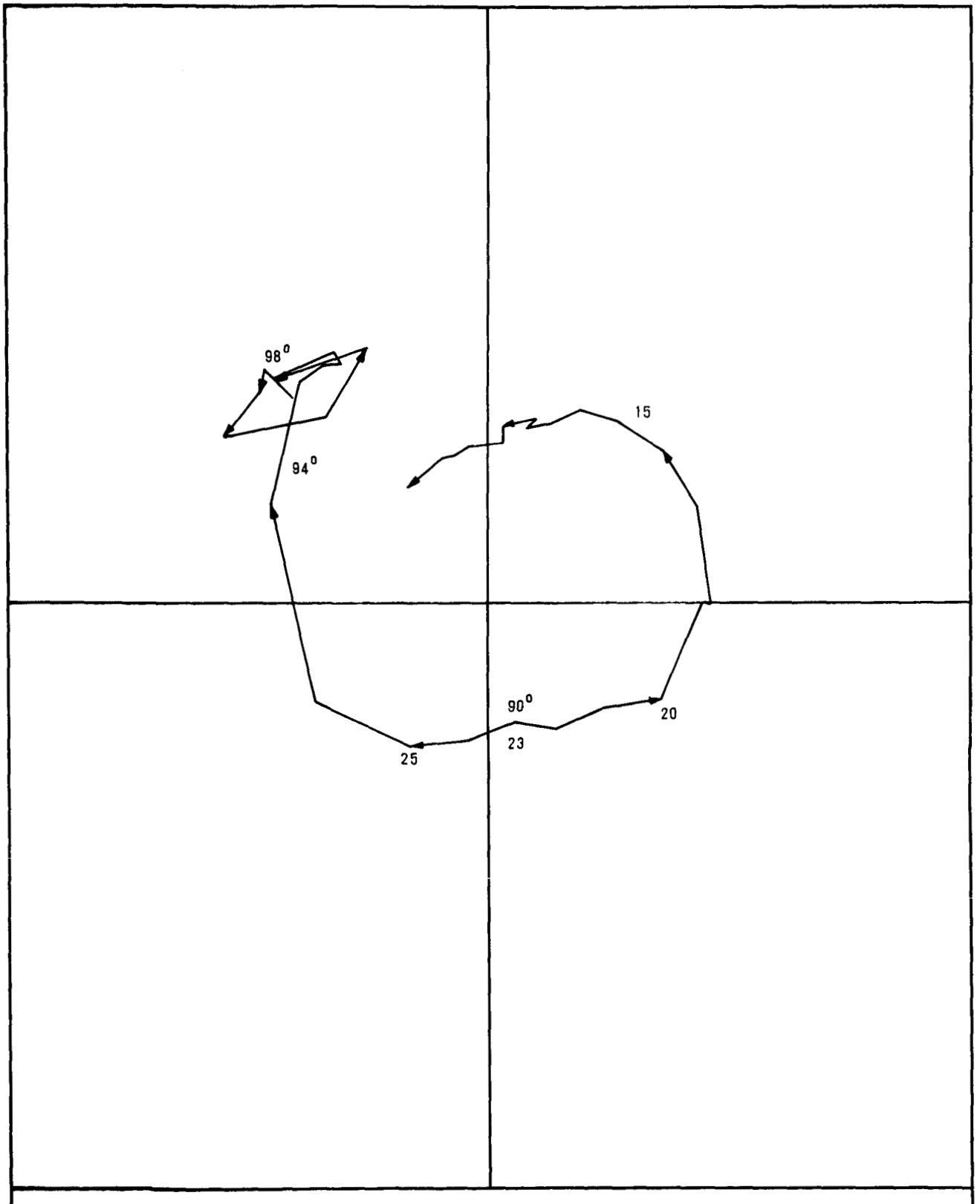

FIG. 4B ABNORMAL COMPONENT FOR JULY 1, 1965 SUNRISE

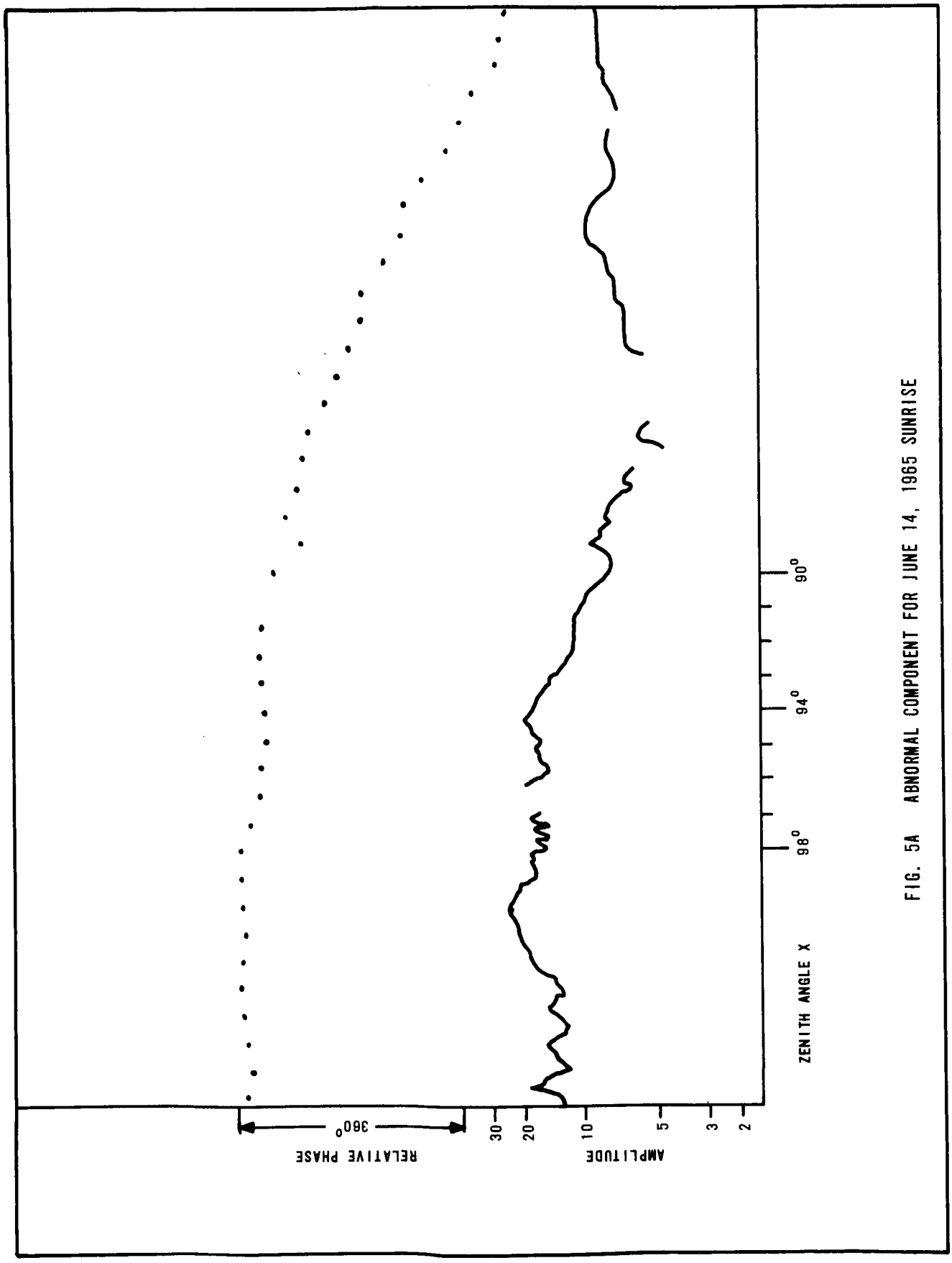

FIG. 5A ABNORMAL COMPONENT FOR JUNE 14, 1965 SUNRISE

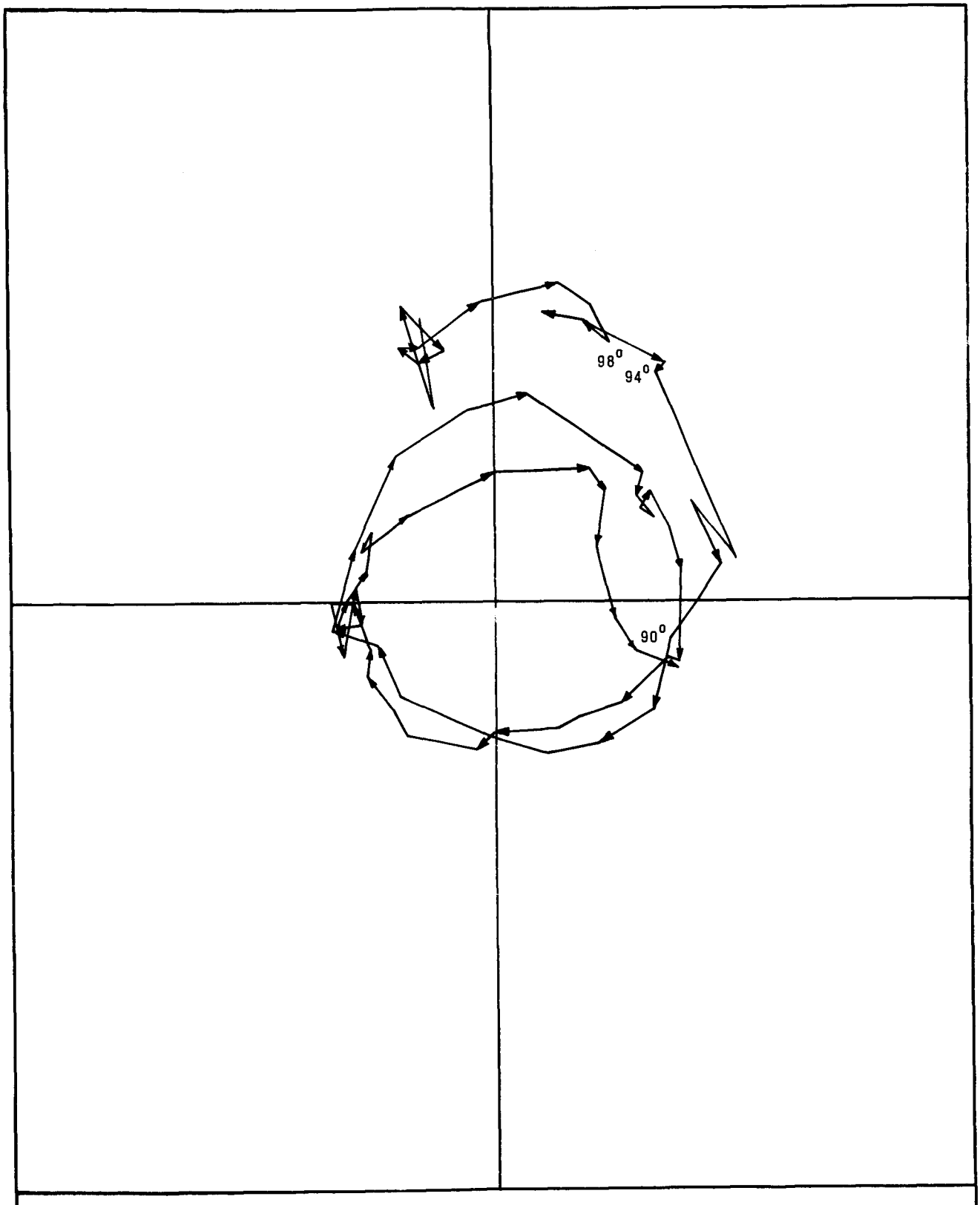

FIG. 5B ABNORMAL COMPONENT FOR JUNE 14, 1965 SUNRISE

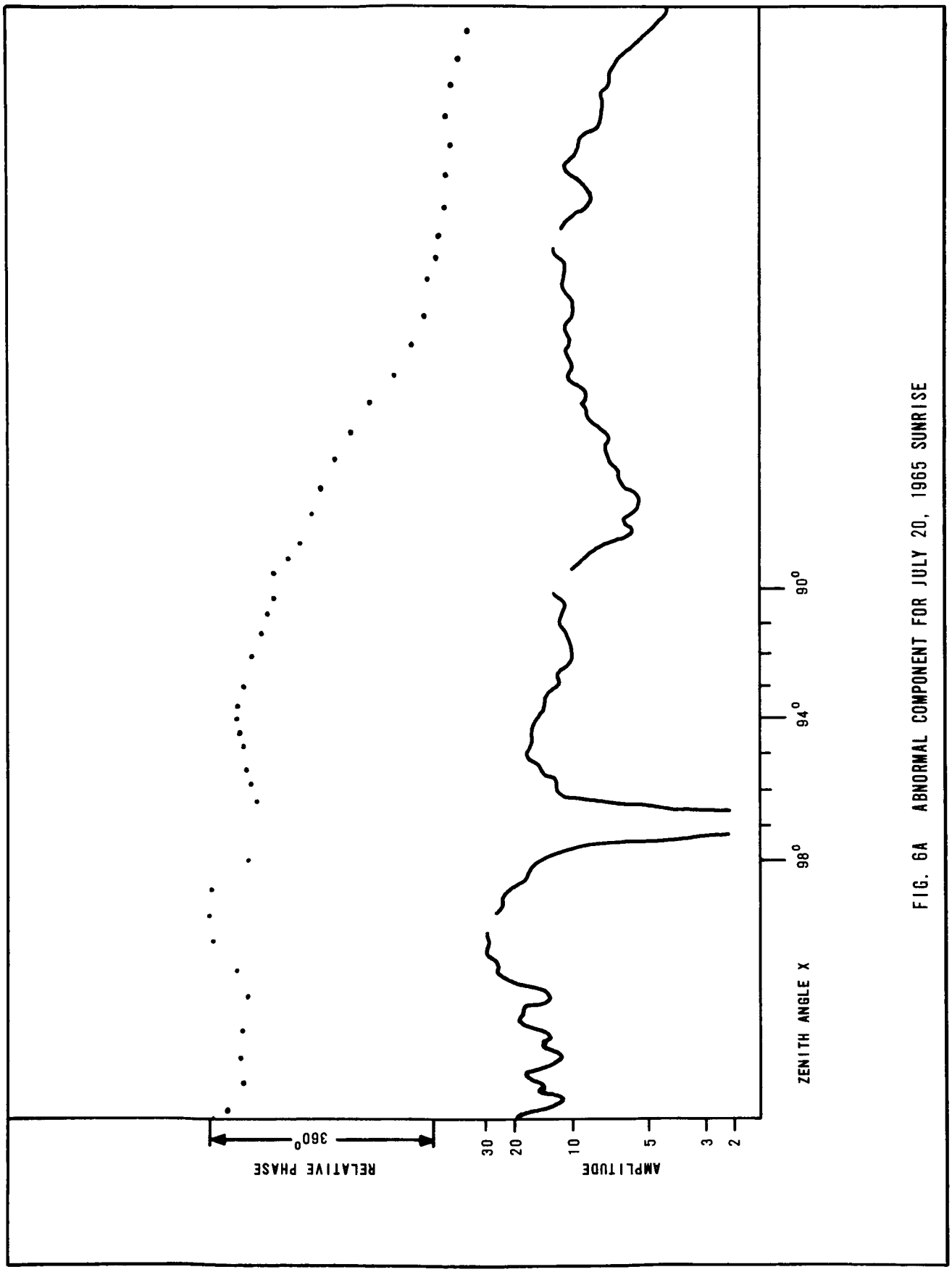

FIG. 6A ABNORMAL COMPONENT FOR JULY 20, 1965 SUNRISE

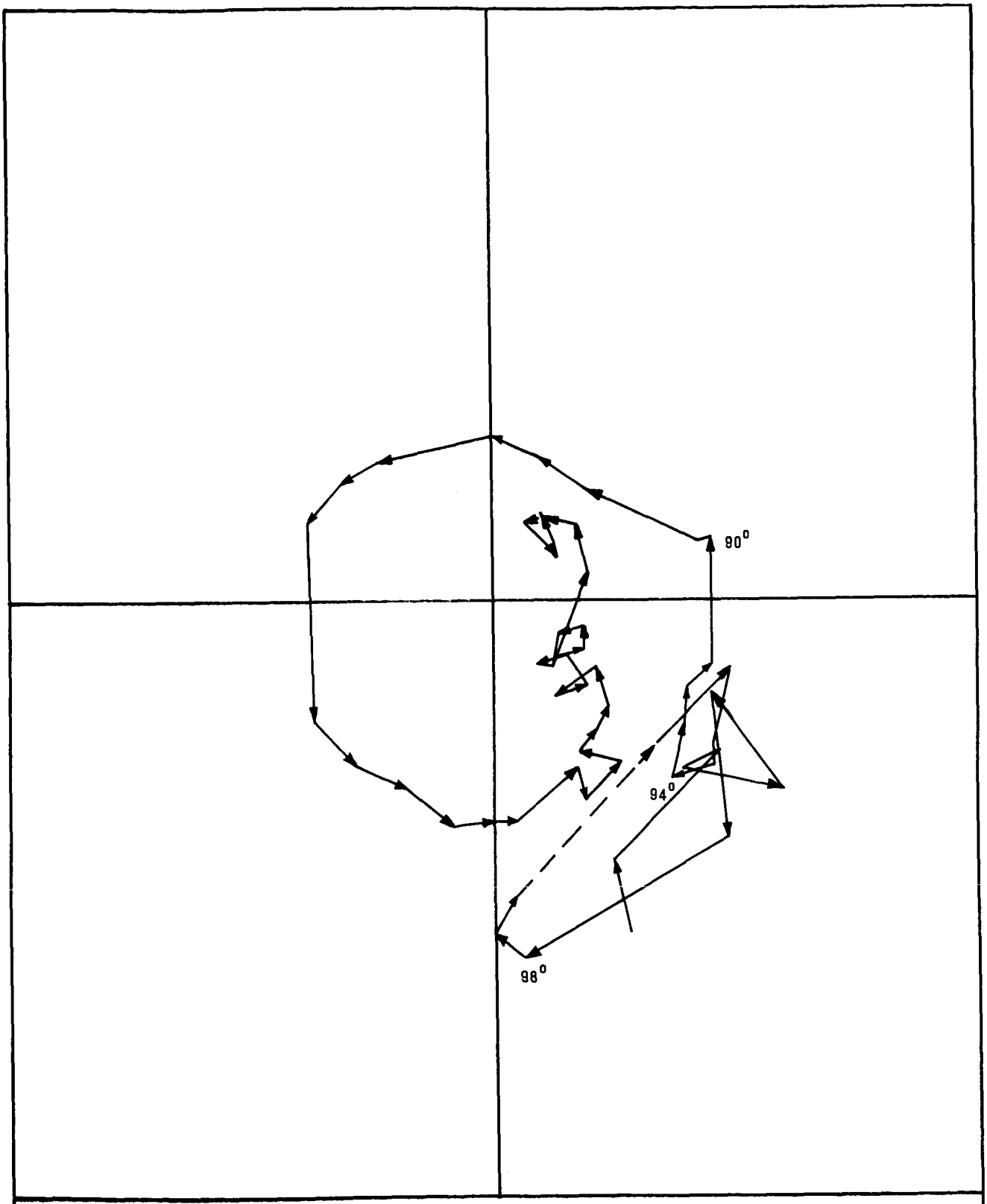

FIG. 6B ABNORMAL COMPONENT FOR JULY 20, 1965

amplitude beginning slightly before $\chi = 99^{\circ}$. This is followed by a further decrease in amplitude beginning at $\chi = 93^{\circ} - 95^{\circ}$, being of the order of 6 db.

Figure 6 is an extreme example of the irregular behavior of the nighttime VLF skywave. On this day the amplitude decreased more than 24 db. On other days this decrease may be about 7 db. The accompanying phase record indicates that after the amplitude recovered, the phase was the same value as before. This indicates that the reflection level did not change and the amplitude decrease was probably due to the interference of two reflected waves. One wave was reflected from the normal nighttime reflection level and the other, a partial reflection, was from a sharp gradient or discontinuity, perhaps from above the normal reflection height.

D. IONIZATION MECHANISMS

Ionization of the normal D-region is produced by solar radiation of three spectral regions. One consists of wavelengths greater than 1900Å and is only capable of ionizing the alkali metals whose abundance is quite small. Second is wavelengths of the range 1100 to 1300Å in which Lyman - α, 1215Å, falls. This is the strongest emission line in the solar spectrum. Lyman - α is capable of ionizing nitric oxide, NO. Also of importance are X-rays, especially during disturbed conditions.

Another important source of ionization is cosmic radiation of galactic origin. Cosmic radiation is independent of solar zenith angle. During the nighttime hours the electrons produced will be removed by attachment, creating a reservoir of negative ions. Evidence points to the existence of negative ions at low levels in the D-region from which electrons are removed during sunrise by photo detachment. These various sources of ionization will be studied briefly.

1. Radio Observations

Many surveys of the diurnal behavior of VLF and LF radio waves have been published. Each essentially points out that about an hour before ground sunrise on short propagation paths the amplitude begins to decrease, but the phase does not begin to advance till near ground sunrise. On longer paths the amplitude decreases similarly but the phase begins to advance at the same time. This has been explained as the result of photodetachment of electrons from O_2^- ions below the nighttime reflection level by visible light of wavelength greater than 3000Å. This is followed by ionization of NO by Lyman - α at ground sunrise. The result is a lower C-layer formed before ground sunrise and the D-layer forming after ground sunrise and blending together of the two layers. The C-layer is traversed by the radio waves on short paths, attenuating the amplitude but not affecting the phase. On longer paths the radio waves are actually reflected from the C-layer, resulting in a pre-sunrise phase advance. Lately, the pre-sunrise variations of phase and amplitude have been studied more closely, resulting in many inconsistencies.

Reid (1964) has analyzed twilight observations of polar-cap absorption of high-frequency galactic noise. If the C-layer were formed by visible light photo detaching O_2^- ions, the changes in absorption would correlate with the

passing of the earth's shadow over the absorbing region, 60 to 90 km. Instead, the absorption follows the passing of the ozone layer's shadow. This indicates the presence of an unknown negative ion, called X^-, whose electron affinity is about 4 ev or at least somewhat more than the .58 ev of O_2^-.

Analysis of steep-incidence VLF data has lead to the conclusion that more than one mechanism is responsible for the pre-sunrise variation of the receiver VLF skywave. There are times when the onset of the sunrise transition occurs at a zenith angle greater than 99^o. A zenith angle of 99^o 40' has been found to be the onset time at oblique incidence by Lauter (1958). The solid earth's shadow reaches 90 km at $\chi = 99^o$ 30' (Figure 7), indicating the presence of O_2^- which is photo detached by visible light. The presence of a screening layer such as a dust layer of variable height of the order of 10 km could explain variances in this onset time.

On many days the onset time of the sunrise transition will be delayed till about $\chi = 98^o$. As a 30 km screening layer (an ozone layer) has its shadow at 90 km when $\chi = 97^o$ 50', this would indicate the presence of the unknown negative ion, X^-, which requires solar ultraviolet light for photo detachment.

Also occurring quite often is an effect which begins at $\chi = 94^o$. This effect has been seen before but usually has been ignored. The usual explanation for this effect is the presence of a two-hop skywave, as well as a one-hop. This will be discussed later. The cause of this effect is not immediately apparent but will be discussed.

Very much has been written about the controversy of O_2^- and X^-. It appears evident that both are present. Which one dominates seems to vary from day to day. Our attention will be on the $\chi = 94^o$ effect and its cause. We will begin by looking at what radiation can cause ionization at D-region levels before ground sunrise.

2. Optical Depth Factor

The determination of the optical depth of the atmosphere for solar zenith angles greater than 90^o has been considered by Swider (1964). For radiation attenuated in a vertical column, the intensity of the radiation $I = I_o e^{-\tau}$, where τ is the optical depth and I_o is the flux where $\tau \approx 0$. The differential optical depth for vertically-incident radiation is defined by

$$d\tau = Kn \cdot dz$$

where K is the absorption cross section of the absorbing medium and K and τ are dependent on the wavelength of the radiation involved, n is the number density of the absorbing medium. The object is to find the integral of this equation.

For a constant scale height atmosphere

$$\tau = K \int_{y=o}^{\infty} n_w e^{-z/h_w} dy$$

where y is the ray path of interest and w is the point of interest. A dimensionless parameter F is defined and called the optical depth factor such that $\tau_w = n_w H_w K F$.

For zenith angles greater than 90^o the optical depth factor must always be found in terms of the point of maximum density along the path y from the sun to P', in terms of point Q' (Figure 8). Therefore

$$\tau (\chi < \pi/2) = Kn_v H_v F_n (U).$$

It is convenient to define U by $\chi = \pi/2 + U$. Tables of $F_n (U)$ are given by Swider and part of these are given here for a scale height, H, of 6 km.

F_n (U) for $\chi > \pi/2$								
U^o	1^o	2^o	3^o	4^o	5^o	6^o	7^o	8^o
F_n	58.8	71.6	78.5	81.1	81.9	82.0	82.1	82.1

The absorption cross section of O_2 for Lyman-α (1215 Å) is only 10^{-20} cm^2 (Watanabe, 1958) and Lyman α penetrates the atmosphere better than other radiation in this wavelength range. At $\chi = 94^o$, when absorption of VLF waves begins, the height where the optical depth is unity is calculated. Most

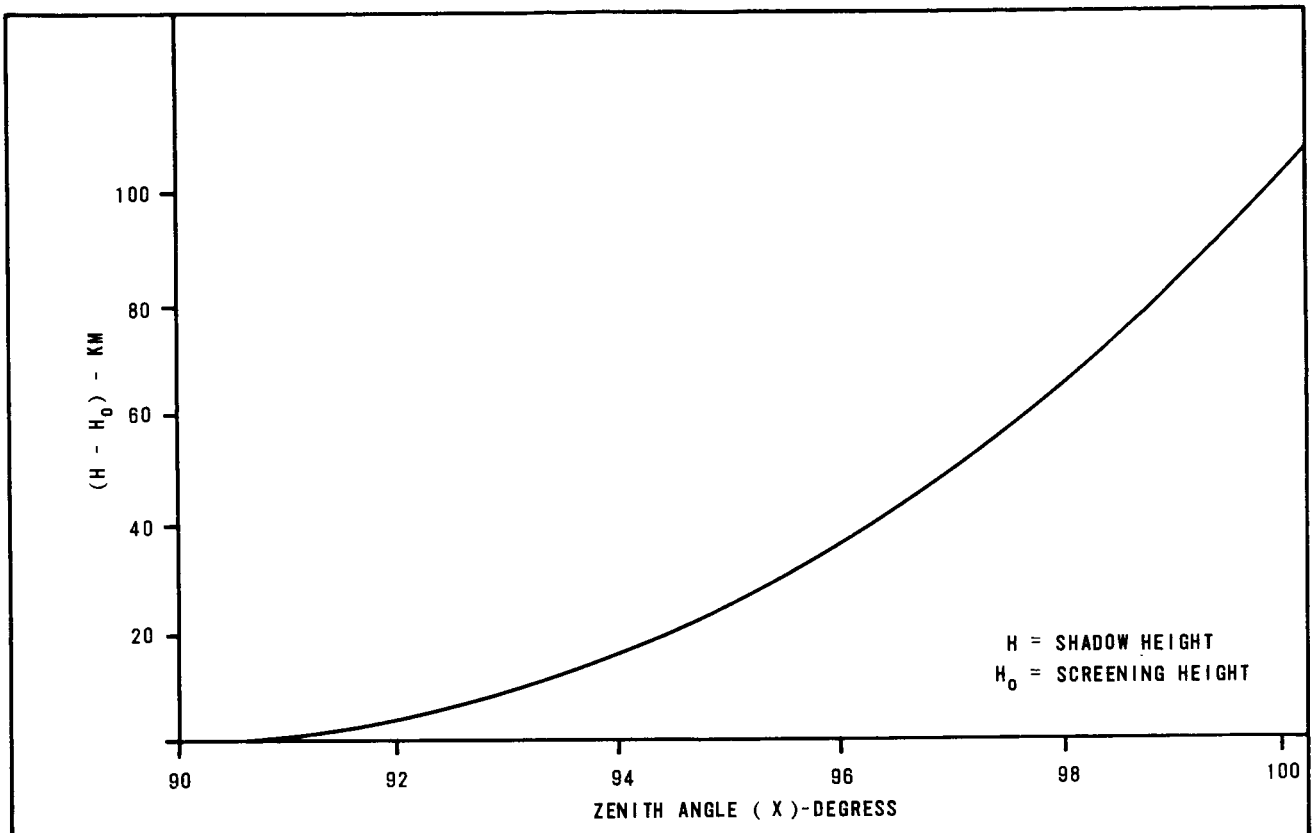

FIG. 7 THE SHADOW HEIGHT OF A SCREENING LAYER

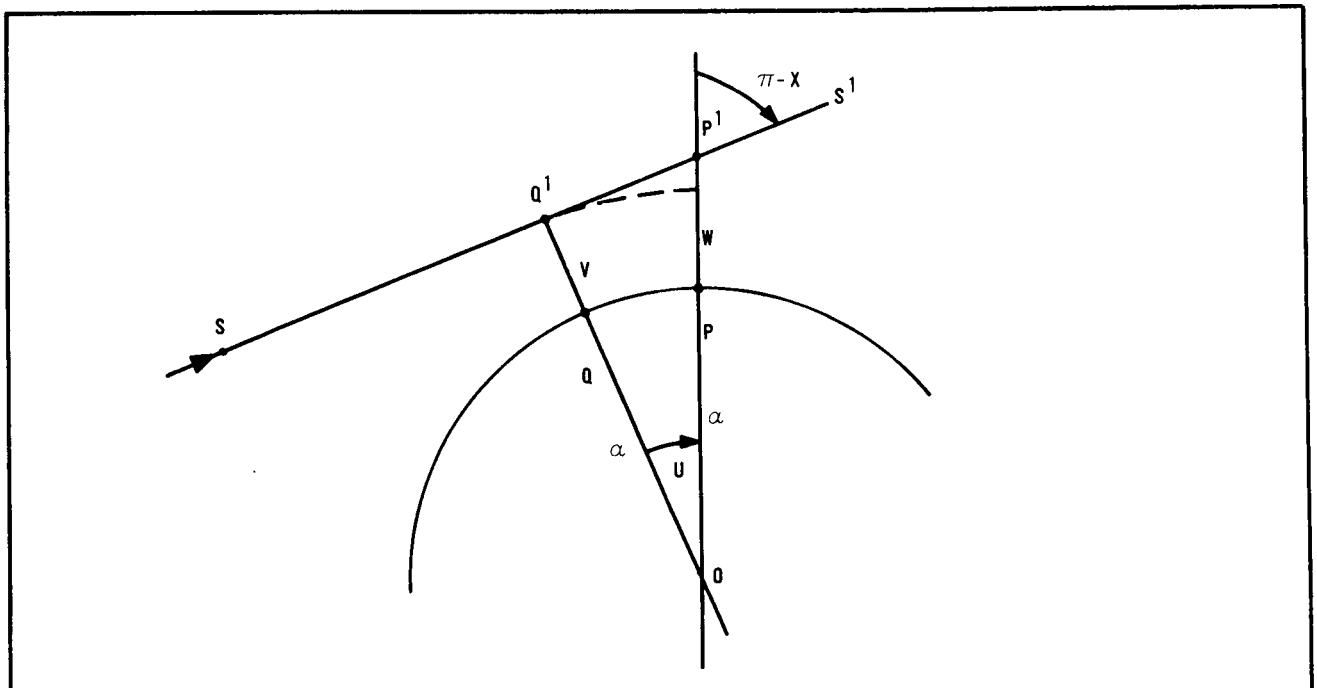

FIG. 8 THE GEOMETRY OF THE EARTH FOR A SOLAR ZENITH ANGLE $X \geq \pi/2$ (SWIDER, 1964)

of the absorption occurs in the region where the optical depth is unity and this height can be used like a screening height. Therefore

$$\tau(\chi = 94^{o}) = 1 = (10^{-20}\ cm^2)\ n_v\ 6.5\ (10^5\ cm) \quad (81.1)$$

$$\therefore\ n_v(O_2) = 1.9\ (10^{12})\ /cm^3 .$$

Taking molecular oxygen to be 21% of the total density of the atmosphere at D-region heights and the Cospar International Reference Atmosphere, 1961, we find a concentration of O_2 molecules of $1.9(10^{12})\ /cm^3$ occurs at a height of 100 km (Figure 9). With this as the screening height, the radiation would only reach 116 km at point P' or at the zenith.

At $\chi = 85^{o}$, the optical depth factor is 9.9; therefore, unit optical depth occurs for Lyman -α at a molecular concentration of

$$n_w = 1.5\ (10^{13})\ cm^{-3}$$

which is only at 89 km.

If we consider ionization by X-rays, the applicable absorption coefficients are 1.3×10^{-19} cm^2 at 10Å and 1.8×10^{-22} at 1Å (Nicolet and Aikin, 1960). At $\chi = 94^{o}$ the concentration of O_2 resulting in unit optical depth is

$$n_v(10\text{Å}) = 1.46\ (10^{11})$$

$$n_v(1\text{Å}) = 1.05(10^{14}).$$

For 10Å radiation this is a screening height of greater than 110 km and a shadow height greater than 126 km. However, for 1Å radiation, the screening height would be 78 km and a shadow of only 94 km. At a zenith angle of 85^{o} the 1Å radiation could reach 65 km.

3. C-Layer Variability

The variability of the C-layer has been seen from the VLF data. This variability has also been measured by Belrose (1962) using the partial reflection technique. Since this layer supposedly is produced by cosmic ray ionization, one might expect large changes in the cosmic ray flux. This, however, is not the

case. Similarly, we cannot cite Lyman -α as the cause. The constancy of Lyman -α flux is well known, even during disturbed and flare conditions. Solar X-rays have been measured by satellites which have shown the extreme variability in the flux of X-rays of wavelength less than 20Å.

The flux of X-rays of wavelength less than 20Å has been measured by NRL satellite SR-1 (Kreplin, et al., 1962) and of wavelength less than 14Å by Injun 1 (Van Allen, 1965). These measurements have revealed a high degree of variability of X-ray flux. For quiet conditions, the solar X-ray flux was measured to be of the order of 10^{-3} erg/cm^2 sec in the 2 to 8Å range. This is two or three orders of magnitude higher than the values used by Nicolet and Aikin. Poppoff and Whitten (1962) have used the new value of the flux to investigate the role of X-rays in the formation of the D-region. They have shown that at a solar zenith angle of 45° and with an estimated solar X-ray spectrum it is possible to produce 100 electrons /cm^3 at an altitude of 70 km.

E. TWO-HOP SIGNAL

It has been suggested that the $\chi = 94^{o}$ effect is merely the result of a two-hop signal being present as well as a one-hop signal. The effect of a two-hop signal has been studied by Bracewell, et al. (1952). The polar diagram of the summation of a one- and a two-hop signal will resemble an epitrochoid, the locus of the sum of two vectors rotating in the same sense. With superscripts used to indicate the order of reflection, a speed factor $G^{(n)}$ gives the speed of of rotation of the n-hop wave relative to the one-hop and is defined as

$$G^{(n)} = \frac{ds^{(n)}}{dh} \Big/ \frac{ds^{(1)}}{dh}$$

where $s^{(n)}$ is the path traveled by the n-hop wave if reflected from height h. For the NSS to Wallops path $G^{(2)}$ is about 2.5. Figure 10 are epitrochoids for a $G^{(2)}$ of 3 when the two-hop signal is 1/4 and 1/2 the one-hop. They are two amplitude minimums 180^{o} apart. The minimums would be 240^{o} apart with $G^{(2)}$ as 2.5. The separation of the minimums, $\Delta\phi = \frac{360}{G^{(2)}-1}$ degrees.

To be sure the effects seen on the abnormal component are the result of changes in the ionosphere and not just a coincidence of the propagation conditions, polar diagrams of the sunrise transitions have been given (Figures 2 to 6). In some cases the presence of the two-hop signal is evident, but not at the correct time to explain the pre-sunrise effects. As nearly all the pre-sunrise variations in amplitude occur before the phase advance begins, the resulting polar diagrams do not describe an epitrochoid during these periods, although after ground sunrise they may.

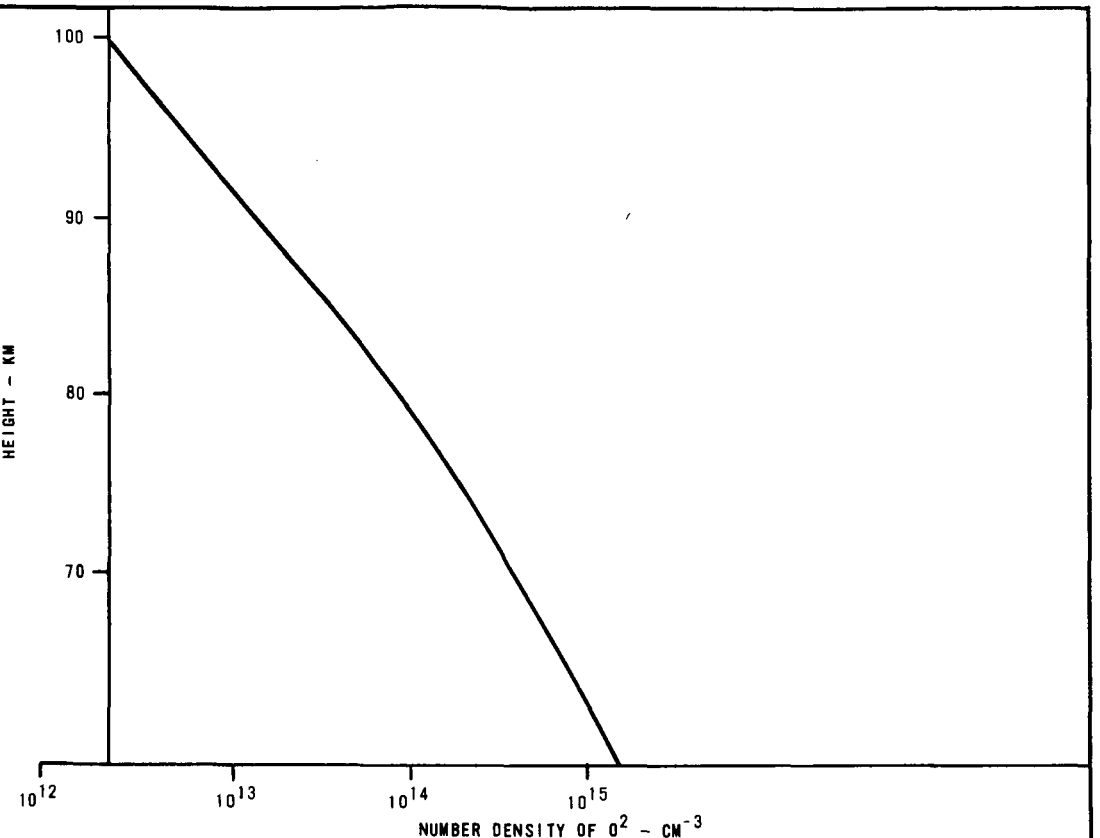

FIG. 9 VARIATION OF O_2 DENSITY WITH HEIGHT

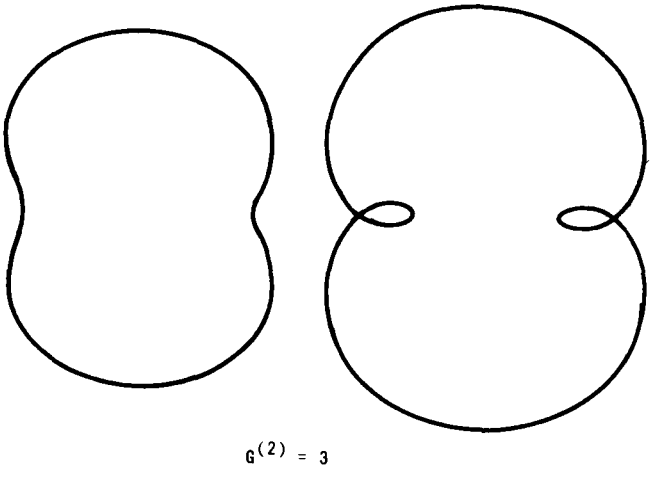

$G^{(2)} = 3$

FIG. 10 EPITROCHOIDS IN WHICH $G^{(2)} = 3$ (BRACEWELL, 1952)

F. SUPPORTING OBSERVATIONS

1. Radio Measurements

Belrose (1962) pointed out a change in slope of the diurnal phase at sunset of 80 kc/s transmissions over a path of 1910 km. At this frequency and path length the radio waves are reflected from the C-region rather than the D-region. On this path the sunset phase retardation begins at approximately the same time the sunrise advance ceased, at about $\chi = 90^{\circ}$. There is a change in slope of the sunset recording at $\chi = 94^{\circ}$ which is not present at sunrise and after this time the phase retardation occurs at a much slower rate until after layer sunset, $\chi = 102^{\circ}$.

Reid (1964) presented curves of measured absorption during a PCA as a function of zenith angle during the sunset twilight period to point out that the dominant negative ion in the D-region must have properties quite different from O_2^-. One can also see (Figure 11) that absorption decreases somewhat erratically until $\chi = 94^{\circ}$ at which time there is a change of slope in the curve and the absorption decreases smoothly until about $\chi = 98^{\circ}$.

2. Rocket Profiles

The most convincing evidence that the effect at $\chi = 94^{\circ}$ is a D-region phenomenon and not merely a consequence of the propagation was presented by Bowhill, et al. (1964). On 15 July 1964 a series of rockets were fired at sunrise. The result was an electron density profile at $\chi = 95^{\circ}$ nearly identical to the nighttime profile. At $\chi = 85^{\circ}$, however, a significant C-layer was present as well as the very beginning of the normal D-layer (Figure 12). This was consistent with the VLF measurements carried out at the same time. The abnormal amplitude began to decrease about $\chi = 94^{\circ}$ and the phase also began to advance slowly. Similarly on 14 June, 1965 the amplitude of the abnormal skywave was watched for a pre-sunrise decrease. The amplitude was nearly constant till $\chi = 94^{\circ}$ at which time it began to decrease rapidly and a D-region rocket was fired. This was accompanied by very little change in phase until after $\chi = 90^{\circ}$. A series of similar rockets were fired in November 1964 at sunrise and sunset. All of these experiments support the fact that the C-layer exists only when the sun's zenith angle is less than 94°.

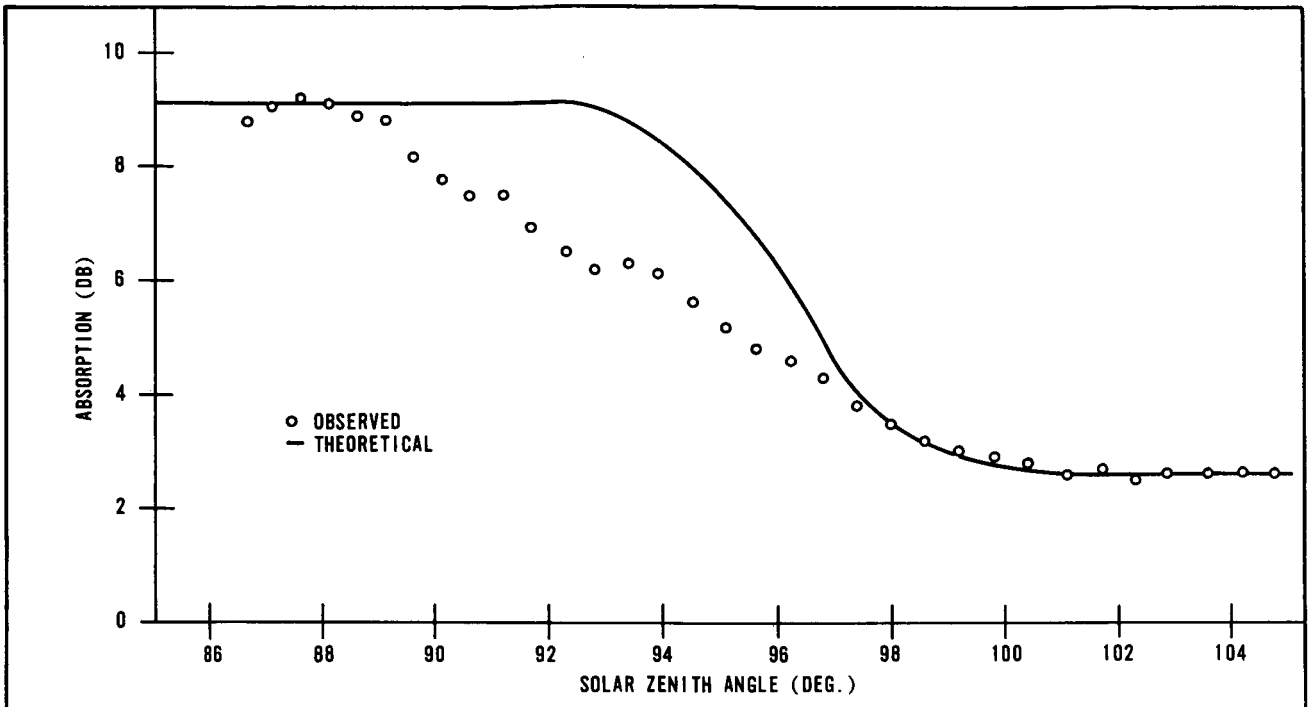

FIG. 11 TWILIGHT VARIATION OF ABSORPTION DURING A PCA EVENT (REID, 1961)

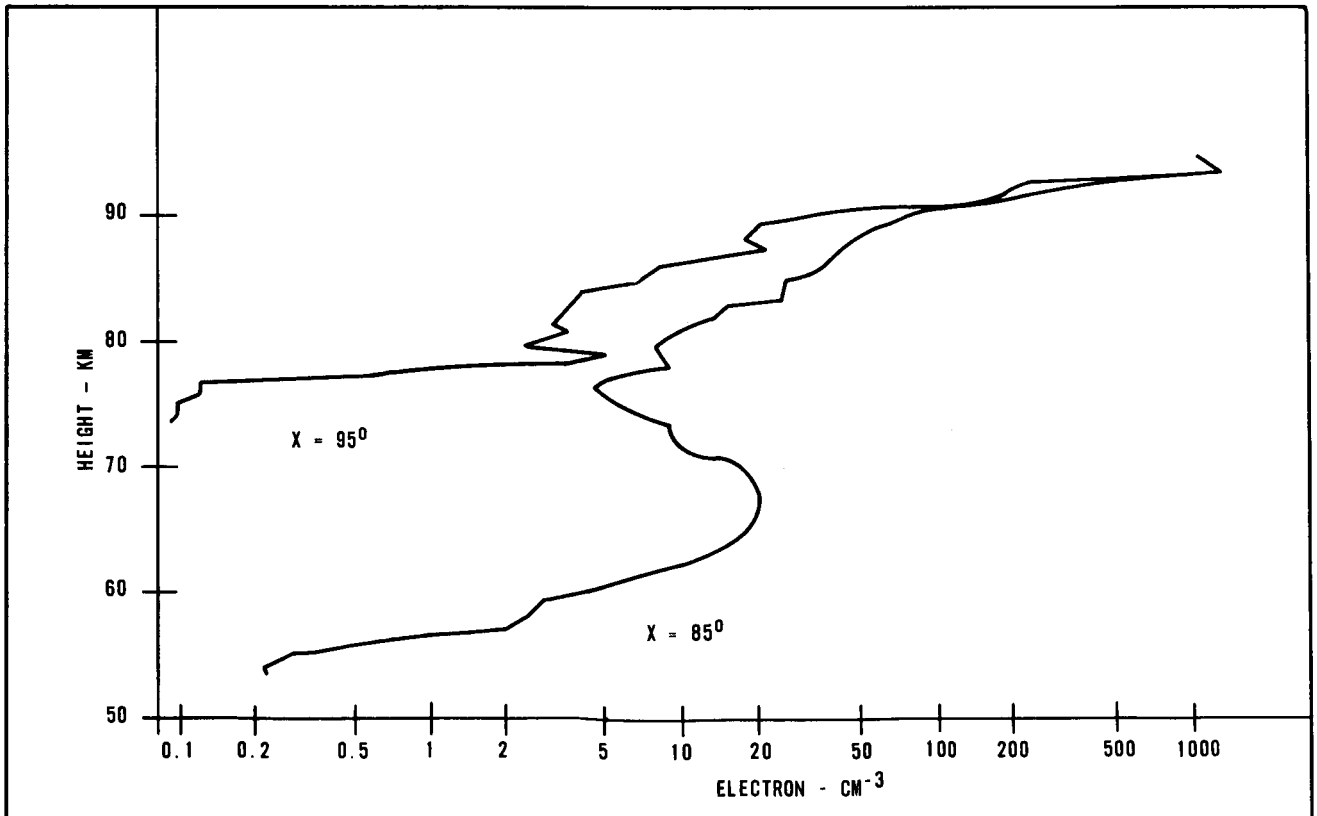

FIG. 12 ELECTRON DENSITY PROFILE FOR 15 JULY 1964 AT WALLOPS ISLAND, VA.

G. SUMMARY

It has been suggested that pre-sunrise ionization of the D-region which forms at a zenith angle of 98° can be attributed to the photo detachment of an unknown negative ion, X^-, by solar ultraviolet light. A screening layer of 30 km is imposed (an ozone layer) which has its shadow at 90 km when $\chi = 97^\circ 50'$. Also suggested is the presence of a negative ion O_2^- which is photodetached by visible light of wavelength greater than 3000A°. It is evident from the VLF recordings that either or both of these mechanisms occur. Each day's recording has some evidence of these mechanisms, although the onset times are somewhat masked by the nighttime variability of the reflected waves. Also evident is an effect beginning at $\chi = 94^\circ$ which appears much more variable in onset time and magnitude. Calculations of the optical depth show that X-rays of wavelength less than 10Å are capable of penetrating below 90 km before ground sunrise. The high variability of solar X-rays has been measured by satellites SR-1.. Measurements have shown the X-ray flux below 10Å varies by an order of magnitude at times; Lyman -α flux remains essentially constant during these times.

H. FULL-WAVE SOLUTION

The propagation of an electromagnetic wave through an ionized medium such as the ionosphere is governed by Maxwell's equations and the constitutive relations of the ionosphere. For studying high-frequency propagation, ray-theory techniques are normally used with the Appleton-Hartree magneto-ionic waves. At low frequencies and especially at VLF these techniques are no longer applicable as the wavelengths are comparable with the thickness of the reflecting region, the D-region. Nor do ray theories include effects of partial reflections which occur when discontinuities and sharp gradients are present in the ionization profile.

If one is to adequately study reflection of LF and VLF radio waves from the ionosphere, the equations governing the propagation must be solved numerically by what is known as a full-wave solution. This solution was first outlined by Budden (1955, 1961) using a digital computer. A similar technique was used for calculating wave fields in the ionosphere by Pitteway (1965).

Neither of the above techniques account for the dependence of the collision frequency on electron energy as was discovered by Phelps and Pack (1959). Seliga (1965) developed a method for calculating wavefields of a LF transmitter as they propagate through the ionosphere, which includes the energy dependence of the collision frequency. This technique has since been adapted for calculation of the VLF reflection coefficients of the ionosphere.

This program has not been completely de-bugged and it is not possible to present results at this time. This program is being written in a manner that will not restrict its use to one computer, one frequency, or one progagation path. It is written in Fortran II-D for an IBM 1620-1443 System. It will accept any frequency, angle of incidence, and the wave normal may make any angle with the earth's magnetic field. The technique is reviewed briefly here.

1. Constitutive Relations

It is assumed that the VLF transmitter is situated on the ground and radiates a plane wave incident on the ionosphere. A cartesian coordinate system is chosen with the z-axis directed vertically upward and the x-z plane includes the wave normal of the incident plane wave.

The constitutive relations of the ionosphere may be written as:

$$[P] = \epsilon_o [M] [E] .$$

In the Appleton Hartree formulation the susceptibility tensor [M] is found to be

$$[M] = - \frac{X}{U(U^2 - Y^2)} \begin{bmatrix} U^2 - Y_x^2 & -iUY_z - Y_xY_y & iUY_y - Y_xY_z \\ iUY_z - Y_yY_x & U^2 - Y_y^2 & -iUY_x - Y_yY_z \\ -iUY_y - Y_zY_x & iUYx - Y_zY_y & U^2 - Y_z^2 \end{bmatrix} .$$

If the energy dependence of the collision frequency is accounted for, it is found that a new variable arises, Z_n. Z_n is related to three complex collision frequency variables, g_n, $n = 1, 2, 3$ where

$$U_n = 1 - iZ_n = 1 - \frac{g_n}{\omega}$$

and

$$g_n = \omega_n \left\{ 5/2 \left(\frac{\omega_n}{\nu_m}\right) C_{5/2}\left(\frac{\omega_n}{\nu_m}\right) - i \left(\frac{\omega_n}{\nu_m}\right)^2 C_{3/2}\left(\frac{\omega_n}{\nu_m}\right) \right\}^{-1} - i\,\omega_n$$

where

$$\omega_{1,2,3} = \omega,\ \omega - \omega_H,\ \omega + \omega_H$$

as shown by Seliga (1965).

$C_{5/2}(y)$ and $C_{3/2}(y)$ are the Dingle integrals defined by

$$C_n(y) = \frac{1}{n!} \int_o^\infty \frac{x^n e^{-x}\, dx}{x^2 + y^2}$$

and have been tabulated by Burke and Hara (1963).

2. Equations of Propagation

The propagation of a plane wave in the ionosphere is governed by Maxwell's equations and the constitutive relations of the ionosphere. When Maxwell's curl equations

$$\nabla \times \bar{E} = -i\omega\mu_o \bar{H}$$

$$\nabla \times \bar{H} = i\omega \bar{D}$$

and the definition of electric polarization

$$\bar{P} = \bar{D} - \epsilon_o \bar{E}$$

are combined with the constitutive relations of the ionosphere, four simultaneous first order differential equations result.

$$E_x' = ik\left[-H_y + \frac{\sin\theta}{1 + M_{zz}}\left(\sin\theta\, H_y + M_{zx}E_x + M_{zy}E_y\right)\right]$$

$$E_y' = ik\, H_x$$

$$H_x' = ik\left[M_{yx}E_x + (1 + M_{yy})\, E_y\right.$$

$$\left. - \frac{Myz}{1 - M_{zz}}\left(\sin\theta\, H_y + M_{zx}E_x + M_{zy}E_y\right) - \sin^2\theta E_y\right]$$

$$H_y' = ik\left[-(1 + M_{xx})E_x - M_{xy}E_y\right.$$

$$\left. + \frac{Mxz}{1 - M_{zz}}\left(\sin\theta\, H_y + M_{zx}E_x + M_{zy}E_y\right)\right]. \qquad (3a)$$

Since each element of the susceptibility tensor [M] is complex, the above set of four equations actually make a set of eight simultaneous first order differential equations, four real and four imaginary.

The other two field quantities are given by

$$E_z = \frac{-1}{1 + M_{zz}} \left[M_{zx} E_x + M_{zy} E_y + \sin\theta \, H_y \right]$$

$$H_z = \sin\theta \, E_y \, . \tag{3b}$$

To solve the simultaneous differential equations, numerical integration is performed simultaneously on the four real and four imaginary equations using a Runge-Kutta process.

A starting solution for the Runge-Kutta process is found by solving the Booker Quartic high in the ionosphere. Above the reflection level, it is assumed that the electron content and collision frequency are constant with height and the only wave present is upgoing. The two solutions of the Booker Quartic with negative imaginary parts correspond to two upgoing waves and are used as initial solutions. The integration is then carried out progressing down through the ionosphere until free space below the ionosphere is reached.

When free space below the ionosphere is reached, any field quantity may be separated into upgoing and downgoing waves, i.e.

$$E_x = U_x + D_x$$

$$\text{and} \qquad E'_x = U'_x + D'_x \, . \tag{4}$$

As the upgoing and downgoing waves U and D vary in free space as

$$U \propto e^{-i k \cos\theta \, z}$$

$$\text{and} \qquad D \propto e^{i k \cos\theta \, z} \tag{5}$$

$$E'_x = -i\,k \cos\theta\ (U_x - D_x)\ . \tag{6}$$

E_x and E'_x results from the numerical integration and therefore

$$U_x = 1/2\left[E_x + \frac{i}{k \cos\theta}\ E'_x\right]$$

$$\text{and} \qquad D_x = 1/2\left[E_x - \frac{i}{k \cos\theta}\ E'_x\right]\ . \tag{7}$$

U_y and D_y are found from similar expressions.

Since we started with two initial solutions above the ionosphere, we have two solutions in free space below the ionosphere. Since the two solutions are independent, the total field is made up of a linear combination of the two solutions. The upgoing incident waves are defined by

$$E_x \text{ inc} = \alpha U_x^{(1)} + \beta U_x^{(2)}$$

$$E_y \text{ inc} = \alpha U_y^{(1)} + \beta U_y^{(2)} \tag{8}$$

where α and β are complex constants and the superscripts (1) and (2) denote the two independent solutions. These two equations may then be solved for α and β in terms of E_x inc and E_y inc.

At VLF the upgoing wave normally has its electric vector in the plane of incidence and the reflection coefficient ($_{\parallel}R_{\parallel}$) and conversion coefficient ($_{\parallel}R_{\perp}$) are desired; these are defined as

$$
\begin{aligned}
{}_{\parallel}R_{\parallel} &= \frac{E_x \text{ down}}{E_x \text{ inc}} \,\Bigg|_{E_y \text{ inc} \,=\, O} = \frac{D_x^{(1)} U_y^{(2)} - D_x^{(2)} U_y^{(1)}}{U_x^{(1)} U_y^{(2)} - U_y^{(1)} U_x^{(2)}} \\
{}_{\parallel}R_{\perp} &= \frac{E_y \text{ down}}{E_x \text{ inc}} \,\Bigg|_{E_y \text{ inc} \,=\, O} = \frac{D_y^{(1)} U_y^{(2)} - D_y^{(2)} U_y^{(1)}}{U_x^{(1)} U_y^{(2)} - U_y^{(1)} U_x^{(2)}} \,.
\end{aligned}
\tag{8}
$$

I. DIURNAL VARIATION

Figure 13 is the diurnal phase and amplitude of the abnormal component for 15 December 1965. A D-region rocket was fired at approximately noon. On this day the amplitude began to decrease at $\chi = 94^{\circ}$. This was accompanied by very little change of phase. The existence of a two-hop signal is suggested by the amplitude minimums at 8:25, 9:55 and 16:50.

For reference, a diagram of the time of occurrence of zenith angles 98°, 94° and 90° is included (Figure 14). Also is shown the time of apparent noon. This is for the NSS-Wallops Island reflection point located at 38° 28'N, 75° 58'W. It is also reasonably accurate for Wallops Station.

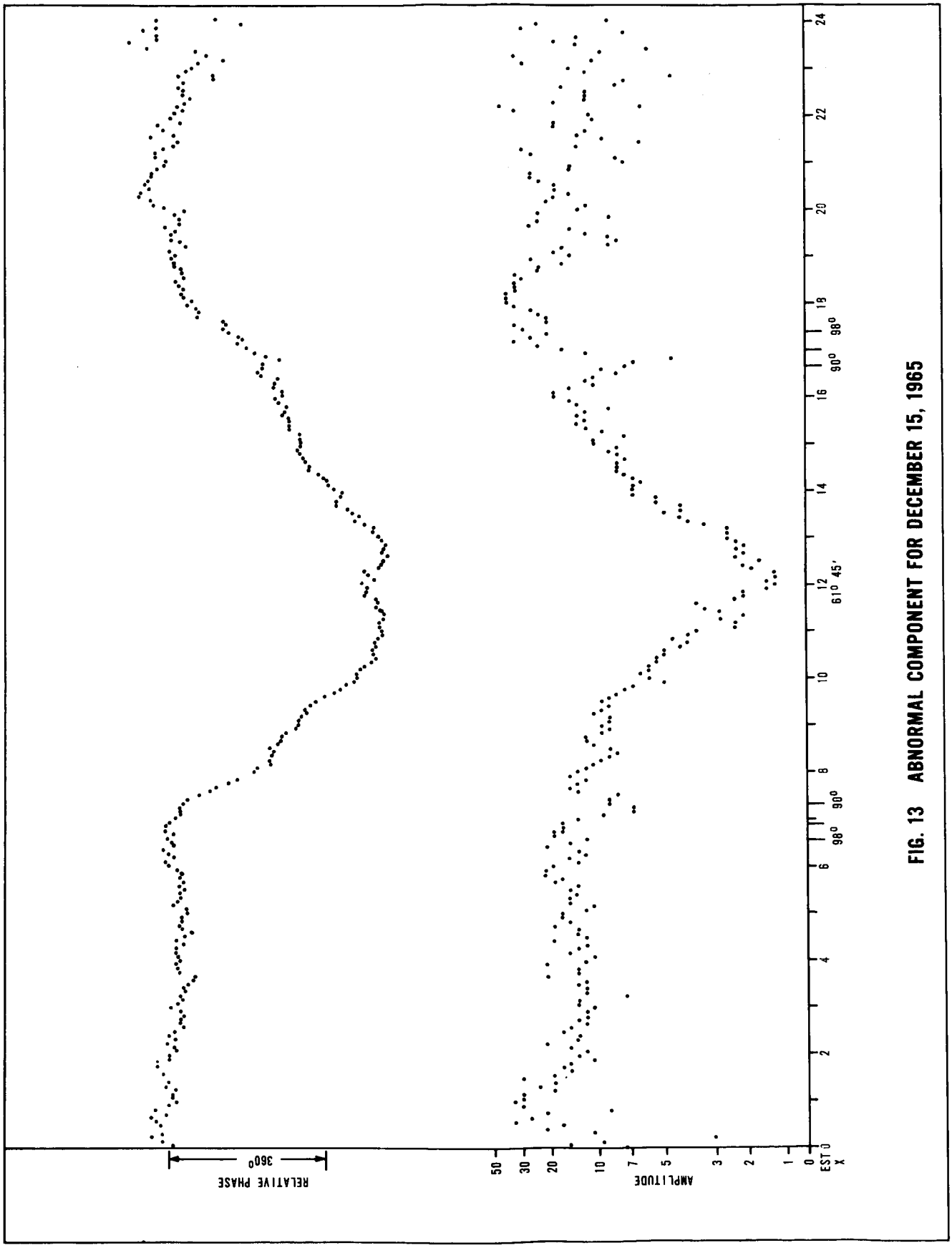

FIG. 13 ABNORMAL COMPONENT FOR DECEMBER 15, 1965

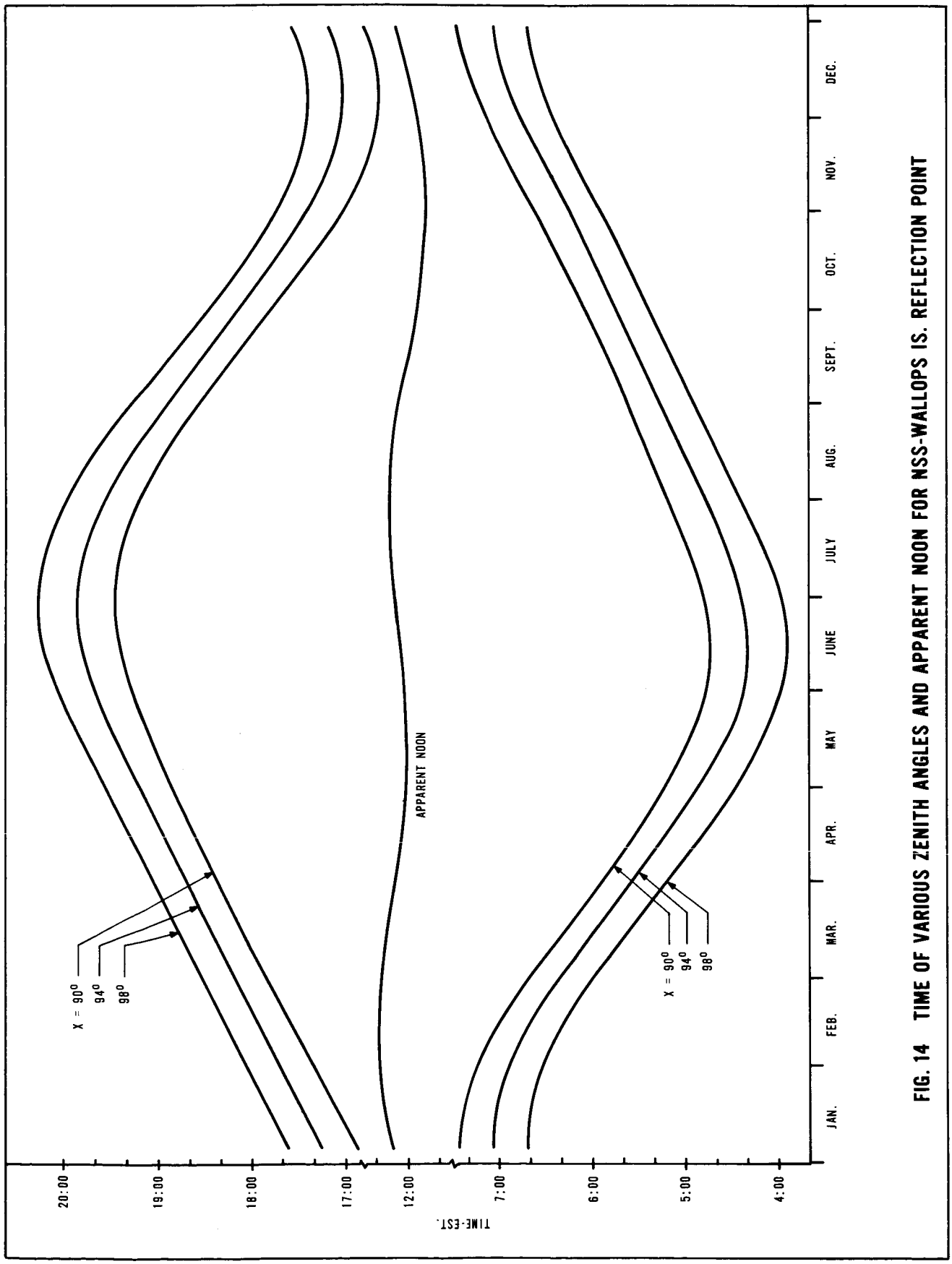

FIG. 14 TIME OF VARIOUS ZENITH ANGLES AND APPARENT NOON FOR NSS-WALLOPS IS. REFLECTION POINT

Reverse (Page 40) Blank

J. CONCLUSIONS

We have examined the sunrise transition of steep-incidence VLF skywaves. The major conclusions of this study are as follows:

1. Recordings of the amplitude and phase of the down-coming VLF skywave have indicated the extreme variability in the formation of the C-layer.
2. Three separate mechanisms which produce a pre-sunrise increase in the lower D-region electron density exist. They are associated with zenith angles of 99^{o} 40', 98^{o}, and 94^{o}.
3. Two species of negative ion appear to exist in the D-region before sunrise, O_2^- and X^-.
4. The effects of X-rays should be studied more closely rather than overlooked in the formation of the C-region.
5. A two-hop signal does not seem able to explain the $\chi = 94^{o}$ effect.
6. D-region rocket experiments have shown conclusively the existence of a D-region ionization mechanism which occurs at $\chi = 94^{o}$.
7. Future study should take two courses:

    a. Detailed analysis of the variation of the reflection coefficient of the ionosphere using full-wave solution of both rocket and model electron density profiles.

    b. A careful analysis of the sources of ionization of the D-region employing latest measurements of radiation flux and reaction rates.

Reverse (Page 42) Blank

REFERENCES

Belrose, J.S., Chapt. 1 & 11, Propagation of Radio Waves at Frequencies Below 300 Kc/s, Pergamon Press, 1964; Edited by W. T. Blackband.

Bowhill, S.A., and G.G. Kleinman, An Integrated Experiment for the Study of the Aeronomy of the D and E Regions of the Ionosphere, Presented at the Fall URSI/IEEE Meeting, 12 - 14 October 1964, Urbana, Illinois.

Bracewell, R.N., The Ionospheric Propagation of Radio Waves of Frequency 16 Kc/s Over Distances of About 200 Km, Proc. I.E.E., 99, Part IV, 217, 1952.

Budden, K.G., The Numerical Solution of Differential Equations Governing Reflection of Long Radio Waves From the Ionosphere, Proc. Roy. Soc. A 227, 516,1955.

Budden, K.G., Radio Waves in the Ionosphere, Cambridge Press, 1961.

Burke, M. J. and E.H. Harra, Tables of the Semiconductor Integrals $C_p(x)$ and Their Approximations for Use With the Generalized Appleton-Hartree Magneto-Ionic Formulas, DRTE Report No. 1113, 1963.

Cospar International Reference Atmosphere, 1961, North Holland Publishing Company.

Kreplin, R.W., T.A. Chubb, and H. Friedman, X-ray and Lyman-Alpha Emissions From the Sun As Measured From the NRL SR-1 Satellite, J. Geophys. Research, 67, 2231, 1962.

Lauter, E.A., and K.H. Schmelovsky, Zur Deutung der Sonnenaufgangseffecte im Langstwillenbereich, Gerlands Beitrage Geophys., 67, 218, 1958.

Nicolet, M., and A.C. Aikin, The Formation of the D-Region of the Ionosphere, J. Geophys., Res., 65, 1469, 1960.

Poppoff, I.G., and R.C. Whitten, D-Region Ionization by Solar X-rays, J. Geophys. Research, 67, 2986, 1962.

Phelps, A.V., and J. L. Pack, Collisional Detachment in Molecular Oxygen, Phys. Rev. Letters, 6, 111, 1961.

Pitteway, M.L.V., The Numerical Calculation of Wave-Fields, Reflexion Coefficients and Polarizations for Long Radio Waves in the Lower Ionosphere, Proc. Roy, Soc. A, 257, 219, 1965.

Reid, G.C., Physical Processes in the D-Region of the Ionosphere, Reviews of Geophys., 2, 311, 1964.

Seliga, T.A., Electron Densities in the D-Region of the Ionosphere From Low-Frequency Signal Strength Measurements in Rockets, Ph.D. Thesis, The Pennsylvania State University, 1965.

REFERENCES (Cont'd)

Swider, W., The Determination of the Optical Depth at Large Solar Zenith Distances, Planet. Space Sci., 12, 761, 1964.

Van Allen, J. A., L. A. Frank, B. Machlum, and L. W. Acton, Solar X-ray Observations by Injun 1, J. Geophys. Res., 70, 1639, 1965.